Electronic Supporting Information (ESI) for

$[CH_3NH_3]_2Ag_4Sn^{IV}_2Sn^{II}S_8$: An Open-Framework Mixed-Valent Chalcogenidostannate

Bo Zhang,[†,‡] Jun Li,[†,‡] Cheng−Feng Du,[†,‡] Mei−Ling Feng,[†] and Xiao−Ying Huang[†,*]

[†] State Key Laboratory of Structural Chemistry, Fujian Institute of Research on the Structure of Matter, Chinese Academy of Sciences, Fuzhou, Fujian, 350002, P. R. China

[‡] University of Chinese Academy of Sciences, Beijing, 100049, P. R. China

Fax: +86 591 63173145; Tel: +86 591 63173145; E-mail: xyhuang@fjirsm.ac.cn

1. Synthesis

The reagents of AgCl (0.143 g, 1 mmol), Sn (0.118 g, 1 mmol), S (0.128 g, 4 mmol) and methylamine (33−40% alcohol solution, 4.0 mL) were sealed in a 23 mL Teflon-lined stainless steel autoclave, heated at 160 °C for 8 days. Then the closed apparatus was taken out from the oven and cooled to room temperature naturally under ambient condition. An orange needle-shaped crystalline product was isolated by filtration (0.094 g, yield ≈34% based on AgCl), washed several times with water and ethanol, and dried under vacuum. EDS analysis gave the average Ag/Sn/S ratio of 1.43: 1.00: 2.40, very close to that determined by the single crystal diffraction. Elemental analysis: calcd. (%) for $[CH_3NH_3]_2Ag_4Sn^{IV}_2Sn^{II}S_8$ (**1**): C 2.17, H 1.09, N 2.53%; found: C 2.30, H 1.09, N 2.50%.

2. Crystal Structure

Single-crystal X-ray diffraction data were collected on a Rigaku MM007−CCD diffractometer with graphite-monochromated MoKα · radiation (λ = 0.71073 Å) at 100 K for compound **1**. The structure of compound **1** was solved by direct methods and refined by full-matrix least-squares on F^2 using the SHELX–2014 program package.[1] Non-hydrogen atoms were refined with anisotropic displacement parameters and the hydrogen atoms attached to the C and N atoms are located at geometrically calculated positions. The empirical formulae were confirmed by the

TGA and EA results. Detailed crystallographic data and structure-refinement parameters of compound **1** are summarized in Table S1.

Table S1 Crystal data and structure refinement parameters for **1**.

Compound	**1**
Empirical formula	$C_2H_{12}Ag_4N_2S_8Sn_3$
Formula weight	1108.17
Crystal system	orthorhombic
Space group	*Pnma*
T/K	100(2)
λ/ Å	0.71073
a/ Å	19.378(9)
b/ Å	7.390(3)
c/ Å	13.683(7)
V/ Å^3	1959.5(16)
Z	4
D_c/ Mg·m^{-3}	3.756
μ/mm^{-1}	8.512
F(000)	2400
Measured refls.	14609
Independent refls.	2390
R_{int}	0.0450
No. of parameters	107
GOF	0.995
[a]R_1, wR_2 [$I > 2\sigma(I)$]	0.0287, 0.0603
R_1, wR_2 (all data)	0.0342, 0.0629

[a]$R_1 = \sum||Fo| - |Fc||/\sum|Fo|$, $wR_2 = \{\sum w[(Fo)^2 - (Fc)^2]^2/\sum w[(Fo)^2]^2\}^{1/2}$

Table S2 Selected bond lengths (Å) and bond angles (°) for **1**.

Sn(1)–S(3)	2.3742(19)	Ag(1)–S(5)	2.6023(15)
Sn(1)–S(1)	2.3928(19)	S(3)–Ag(1)#4	2.5672(13)
Sn(1)–S(2)#4	2.4163(14)	S(5)–Ag(1)#1	2.6022(15)
Sn(1)–S(2)	2.4164(14)	Ag(1)–Ag(1)#1	3.1127(17)
Sn(2)–S(4)	2.5193(19)	Ag(1)–Ag(2)	3.2283(13)
Sn(2)–S(2)#5	2.5675(14)	Ag(2)–S(1)	2.5564(15)
Sn(2)–S(2)#4	2.5675(14)	Ag(2)–S(6)	2.4547(16)
S(2)–Sn(2)#9	2.5676(14)	Ag(2)–S(1)#2	2.7753(14)
Sn(3)–S(4)	2.425(2)	S(1)–Ag(2)#4	2.5563(15)
Sn(3)–S(5)	2.3918(19)	S(1)–Ag(2)#2	2.7753(14)
Sn(3)–S(6)#7	2.3874(14)	S(1)–Ag(2)#8	2.7753(14)
Sn(3)–S(6)#6	2.3873(14)	Ag(2)–Ag(2)#4	3.0436(17)
S(6)–Sn(3)#10	2.3874(14)	Ag(2)–S(2)#3	2.8887(18)
Ag(1)–S(6)	2.5534(17)	S(2)–Ag(2)#8	2.8887(18)

Ag(1)–S(3)	2.5672(13)		
S(3)–Sn(1)–S(2)	111.44(4)	S(6)#6–Sn(3)–S(4)	105.83(4)
S(1)–Sn(1)–S(2)	104.25(4)	S(6)#7–Sn(3)–S(4)	105.83(4)
S(3)–Sn(1)–S(2)#4	111.44(4)	S(5)–Sn(3)–S(4)	113.60(5)
S(1)–Sn(1)–S(2)#4	104.25(4)	S(6)#6–Sn(3)–S(5)	107.67(4)
S(3)–Sn(1)–S(1)	118.05(6)	S(6)–Ag(1)–S(3)	119.98(5)
S(2)#4–Sn(1)–S(2)	106.52(7)	S(6)–Ag(1)–S(5)	108.33(5)
S(4)–Sn(2)–S(2)#5	94.07(4)	S(3)–Ag(1)–S(5)	116.48(5)
S(4)–Sn(2)–S(2)#4	94.07(4)	S(6)–Ag(2)–S(1)	141.87(5)
S(2)#5–Sn(2)–S(2)#4	86.47(6)	S(6)–Ag(2)–S(1)#2	113.60(5)
S(6)#6–Sn(3)–S(6)#7	116.44(7)	S(1)–Ag(2)–S(1)#2	88.51(4)
S(6)#7–Sn(3)–S(5)	107.67(4)	S(1)#2–Ag(2)–S(2)#3	84.14(5)

Symmetry transformations used to generate equivalent atoms: for **1** #1 *x*, –*y*+3/2, *z* #2 –*x*+1, –*y*+1, –*z*+1 #3 –*x*+1, *y*+1/2, –*z*+1 #4 *x*, –*y*+1/2, *z* #5 *x*, *y*+1, *z* #6 –*x*+1/2, *y*+1/2, *z*–1/2; #7 –*x*+1/2, –*y*+1, *z*–1/2 #8 –*x*+1, *y*–1/2, –*z*+1 #9 *x*, *y*–1, *z* #10 –*x*+1/2, –*y*+1, *z*+1/2.

Table S3 Selected Hydrogen Bonds Data for **1**.

D–H···A	D–H (Å)	H···A (Å)	D···A (Å)	<(DHA) (°)
N(2)–H(2A)···S(6)#11	0.91	2.81	3.384(6)	122.4
N(2)–H(2B)···S(5)#7	0.91	2.84	3.585(8)	140.4
N(2)–H(2B)···S(6)#7	0.91	2.82	3.384(6)	120.9
N(2)–H(2C)···S(3)	0.91	2.65	3.357(8)	135.2
N(1)–H(1)···S(2)#12	0.91	2.72	3.525(5)	147.6
N(1)–H(2)···S(6)#11	0.91	2.65	3.279(5)	126.9
N(1)–H(3)···S(3)	0.91	2.65	3.374(6)	137.6
N(1)–H(3)···S(6)#7	0.91	2.83	3.279(5)	111.6

Symmetry transformations used to generate equivalent atoms: for **1** #1 *x*, –*y*+3/2, *z* #2 –*x*+1, –*y*+1, –*z*+1 #3 –*x*+1, *y*+1/2, –*z*+1 #4 *x*, –*y*+1/2, *z* #5 *x*, *y*+1, *z* #6 –*x*+1/2, *y*+1/2, *z*–1/2; #7 –*x*+1/2, –*y*+1, *z*–1/2 #8 –*x*+1, *y*–1/2, –*z*+1 #9 *x*, *y*–1, *z* #10 –*x*+1/2, –*y*+1, *z*+1/2 #11 –*x*+1/2, *y*–1/2, *z*–1/2 #12 *x*–1/2, –*y*+1/2, –*z*+1/2.

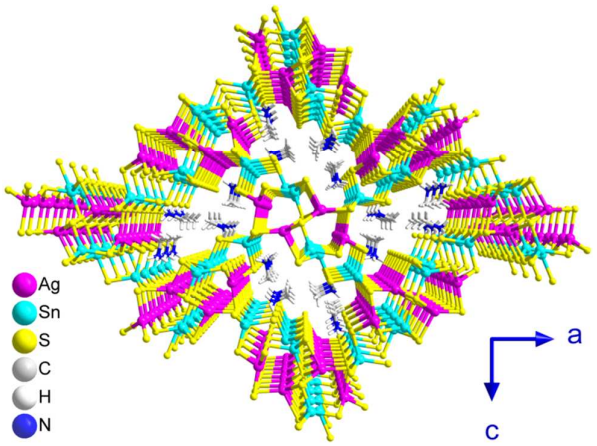

Figure S1. Perspective view of the structure of compound **1** along the *b* axis showing the 1D channels filled with the protonated $[CH_3NH_3]^+$ cations.

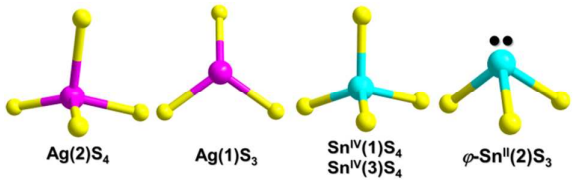

Figure S2. The coordination modes of Ag^+, Sn^{4+} and Sn^{2+} ions in compound **1**.

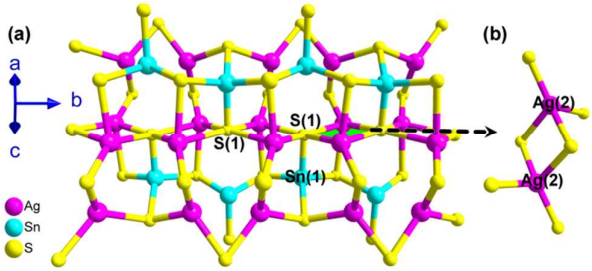

Figure S3. (a) The $[Ag_4Sn^{IV}Sn^{II}S_8]_n^{6n-}$ ribbon showing the S(1) atoms and the $[Ag_2S_2]$ rings. (b) The $[Ag_2S_2]$ ring.

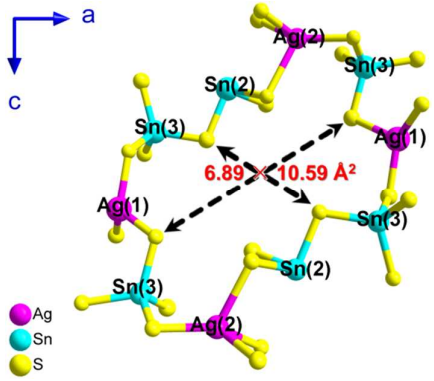

Figure S4. The window of channel extending along the *b* axis in compound **1**.

It deserves to be specially noted that in the $[Ag_4Sn^{IV}Sn^{II}S_8]_n^{6n-}$ ribbon, the S(1) atoms adopt an infrequent μ_5-quadrangular pyramidal geometry to bond four Ag(2)

and one Sn(1) atoms (Figure S3). The channels parallel to the *b* axis are distorted cross-shaped with a cross-section of 6.89 × 10.59 $Å^2$, which are composed of a 20-membered ring defined by two [AgS_3], two [AgS_4], four [SnS_4] and two [SnS_3] units via corner-sharing (Figure S4).

3. BVS Calculation

The valence sum = $\sum$exp[(d_0–d)/B], d_0 = 2.45 for Sn–S, B = 0.37;[2]

(1) Four values of $d_{(Sn(1)–S)}$ are 2.3742, 2.3928, 2.4163 and 2.4164, respectively.

The valence sum = exp[(2.45–2.3742)/0.37] + exp[(2.45–2.3928)/0.37] + exp[(2.45–2.4163)/0.37] + exp[(2.45–2.4164)/0.37] = 4.585

(2) Three values of $d_{(Sn(2)–S)}$ are 2.5193, 2.5675 and 2.5675, respectively.

The valence sum = exp[(2.45–2.5193)/0.37] + exp[(2.45–2.5675)/0.37] + exp[(2.45–2.5675)/0.37] = 2.285

(3) Four values of $d_{(Sn(3)–S)}$ are 2.425, 2.3918, 2.3874 and 2.3874, respectively.

The valence sum = exp[(2.45–2.425)/0.37] + exp[(2.45–2.3918)/0.37] + exp[(2.45–2.3874)/0.37] + exp[(2.45–2.3874)/0.37] = 4.609

4. Physical Measurements

Elemental analyses of C, H, and N were performed using a German Elementary Vario EL III instrument. Energy-dispersive spectroscopy (EDS) was recorded on a JEOL JSM-6700F scanning electron microscope. Thermogravimetric analyses were carried out with a NETZSCH STA449C at a heating rate of 10 °C/min under a nitrogen atmosphere. Powder X-ray diffraction (PXRD) patterns were collected at room temperature on a Miniflex II diffractometer using Cu Kα radiation (λ = 1.5406 Å) in the 2θ range of 5−50°. Room-temperature optical diffuse reflectance spectrum of powder samples was obtained using a UV−vis−NIR Varian 86 Cary 500 Scan spectrophotometer. Absorption (α/S) data were calculated from reflectance using the Kubelka−Munk function $\alpha/S = (1 - R)^2/2R$, where α is the absorption coefficient, S is the scattering coefficient which is practically independent of wavelength when the particle size is larger than 5 μm, and R is the reflectance.[3a] For a crystalline semiconductor with an indirect band gap, its optical absorption near the band edge follows the equation given by Tauc, $(\alpha E)^{1/2} = A(E - E_g)$, where α is the absorption coefficient, A is the proportionality constant, E is the photon energy, and E_g is the optical band gap.[3b] Fourier transform infrared (FT−IR) spectrum was taken on a

Nicolet Magna 750 FT−IR spectrometer in the 4000−400 cm^{-1} region by using a KBr pellet. XPS experiments were carried out on an ESCALAB 250Xi spectrometer with Al Kα radiation as X-ray source for radiation. The supernate of photocatalytic experiment was analyzed with the help of UV−vis absorption spectra instrument (SHIMADZU UV-2600 UV−vis spectrometer).

(1) EDS

Data collected from five points on the surface of one single crystal of **1** confirmed that the average Ag: Sn: S ratio was 1.43: 1.00: 2.40, very close to that determined by the single crystal diffraction.

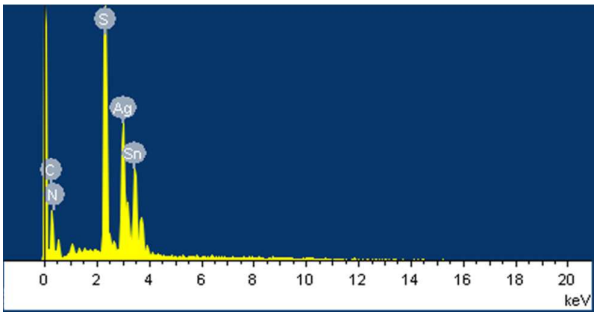

Figure S5. The energy dispersive X-ray (EDX) spectrum of **1**.

(2) PXRD

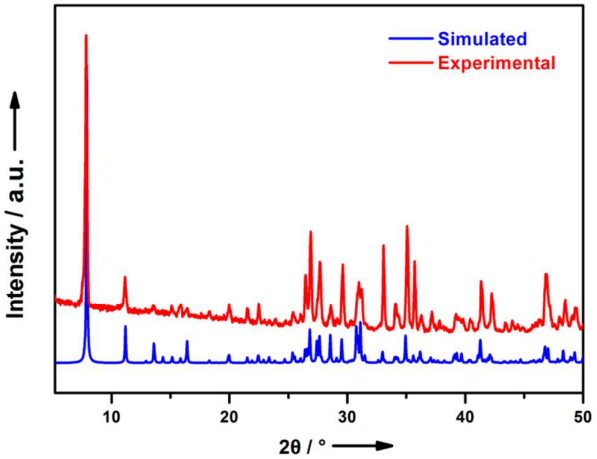

Figure S6. Experimental and simulated PXRD patterns of **1**.

(3) TGA

The TG curve of compound **1** (Figure S7) displays one main step weight loss of 8.51% (theoretical value of 8.68%) in the range of 244−590 °C, corresponding to the loss of two CH_3NH_2 and one H_2S molecule per formula. With increasing the temperatures, the progressive weight loss observed in compound **1** continued and still

did not achieve the balance at 800 ℃.

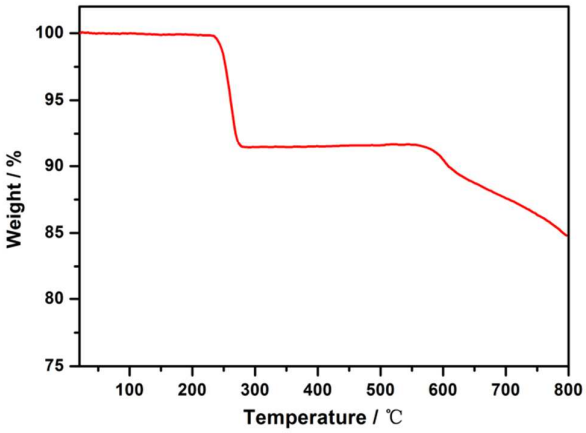

Figure S7. Thermogravimetric curve for **1**.

(4) FT-IR spectrum

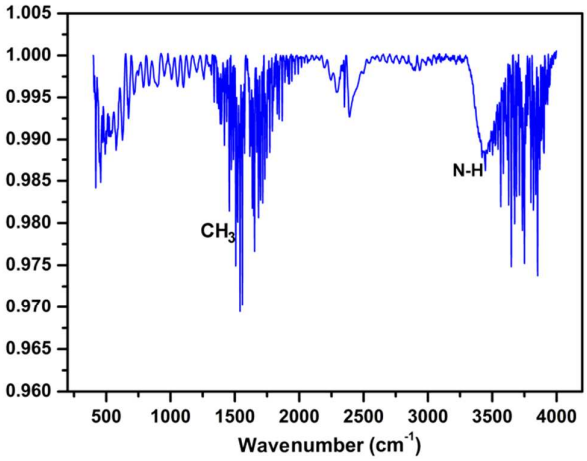

Figure S8. FT−IR spectrum of compound **1**.

(4) Photocatalytic Activity for Degradation of CV

The photocatalytic activity of compound **1** for the degradation of CV was evaluated under the visible light irradiation of a 300 W Xe lamp equipped with a cutoff filter (λ > 420 nm). The distance between the Xe lamp and the reaction vessel was ~20 cm. In a typical photocatalytic reaction, 30 mg of photocatalyst was suspended in 50 ml of CV solution (1.0×10^{-5} M). Prior to visible light illumination, the suspension was magnetically stirred in the dark for 30 min to reach an adsorption–desorption equilibrium between the photocatalyst and solution. After each 40 min intervals, 4 mL

of CV solution was removed from the system for analysis. After 240 min of photoreaction, the suspension was centrifugalized at a speed of 9000 rpm/min for 5 min, and the resulting solution was analyzed on a SHIMADZU UV-2600 UV−vis spectrometer. Meanwhile, a blank experiment in the absence of the photocatalyst was also performed under identical conditions, and the corresponding CV aqueous solution was dealt with via the above-mentioned method.

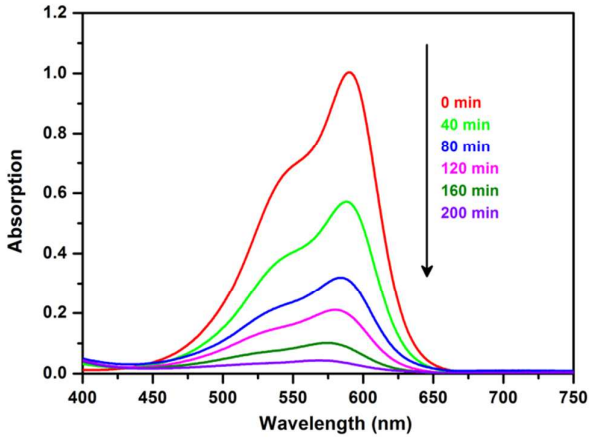

Figure S9. Absorption spectra of a solution of CV in the presence of compound **1** under exposure to visible light.

PXRD indicated that compound **1** can keep its crystallinity after immersion in aqueous solutions of CV, presented in Figure S10.

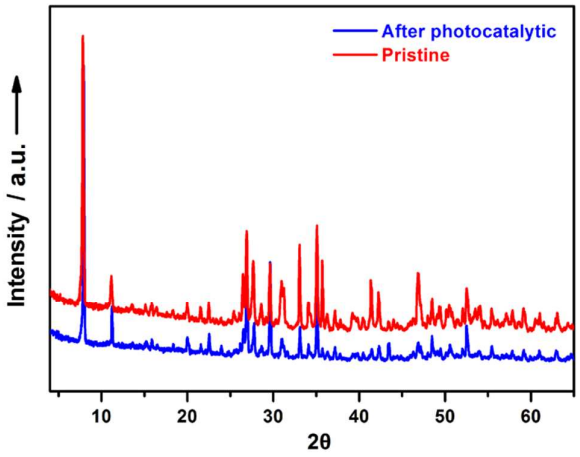

Figure S10. PXRD patterns of compound **1** before and after the photocatalytic process.

(5) Theoretical Calculations

Single-crystal structural data of compound **1** was used for the theoretical calculation. The present calculation was performed in the DFT framework,

implemented in the CASTEP package.[4] The Perdew-Burke-Ernzerhof (PBE) functional of the generalized gradient approximations (GGA) was employed as the exchange-correlation functional.[5] The valence atomic configurations were $1s^2$, $2s^22p^2$, $2s^22p^3$, $3s^23p^4$, $4d^{10}5s^1$ and $5s^25p^2$, for H, C, N, S, Ag and Sn, respectively. The number of plane waves included in the basis was determined by a cutoff energy of 400 eV, and the numerical integration of the Brillouin zone was performed using a 1 × 3 × 2 Monkhorst−Pack *k*-point.

DFT calculations on the band structure indicated compound **1** is an indirect semiconductor with a band gap of 1.27 eV (Figure S11), which is smaller than the experimental value of 2.10 eV. As is well-known, such a discrepancy between the experimental and calculated band gap is due to the inaccurate description of eigenvalues of the electronic states by generalized gradient approximation (GGA),[5b] which often causes quantitative underestimation of the band gaps for semiconductors and insulators.[6] Further calculations on the partial density of states reveal that the conduction bands (CBs) above the Fermi level (the Fermi level is set at 0 eV) are mainly made up of S-3p, Sn-5s and Sn-5p states, whereas the valance bands (VBs) just below the Fermi level are mainly derived from Ag-4d, S-3p and Sn-5p states (Figure S12).

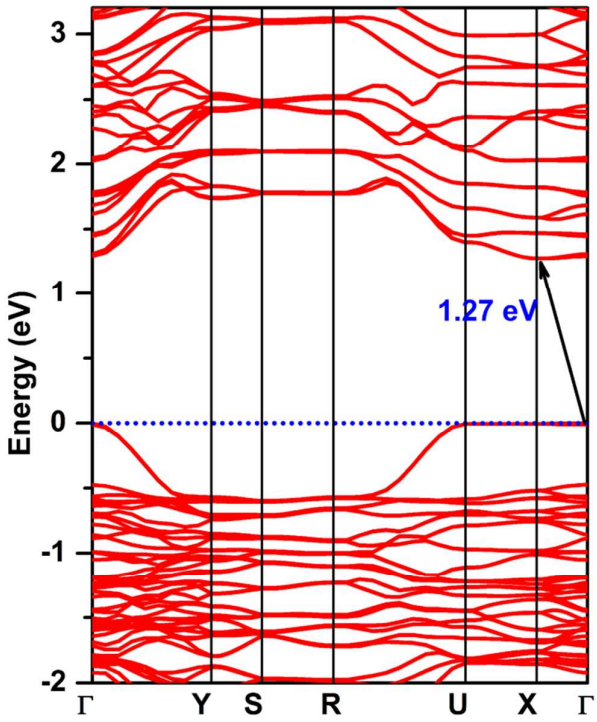

Figure S11. The band structure of compound **1**. Fermi level is set at 0 eV (dot line).

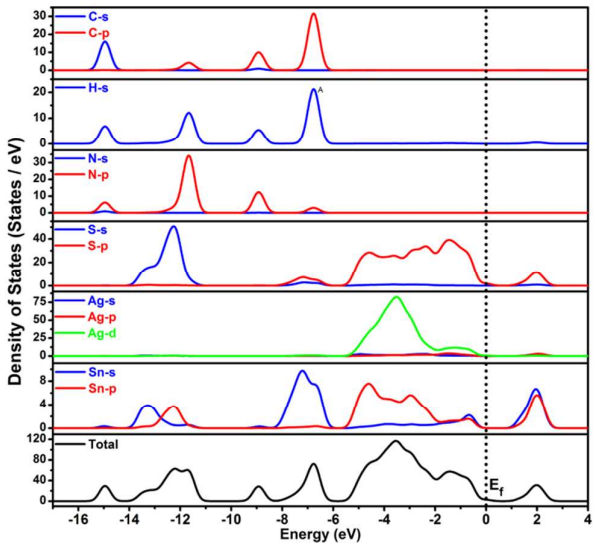

Figure S12. The total density of states and partial density of states of **1**. Fermi level is set at 0 eV (dashed line).

References

1. Sheldrick, G. M. Crystal Structure Refinement with SHELXL. *Acta Cryst.* **2015**, *71*, 3–8.
2. Brese, N. E.; Okeeffe, M. Bond-Valence Parameters for Solids. *Acta Crystallogr.,*

Sec. B: Struct. Sci, **1991**, *47*, 192–197.

3. (a)Wendlandt, W. W.; Hecht, H. G. *Reflectance Spectroscopy*; Interscience, New York, 1966. (b) Tauc, J.; Grigorovici, R.; Vancu, A. Optical Properties and Electronic Structure of Amorphous Germanium. *Phys. Status Solidi B*, **1966**, *15*, 627–637.
4. Segall, M. D.; Lindan, P. J. D.; Probert, M. J.; Pickard, C. J.; Hasnip, P. J.; Clark, S. J.; Payne, M. C. First-Principles Simulation: Ideas, Illustrations and the CASTEP Code. *J. Phys.: Condens. Matter,* **2002**, *14,* 2717–2744.
5. (a) Perdew, J. P.; Burke, K.; Ernzerhof, M. Generalized Gradient Approximation Made Simple. *Phys. Rev. Lett.*, **1996**, *77*, 3865–3868. (b) Kresse, G.; Furthmuller, J. Efficient Iterative Schemes for AB Initio Total-Energy Calculations Using a Plane-Wave Basis Set. *Phys. Rev. B: Condens. Matter*, **1996**, *54*, 11169–11186.
6. (a) Godby, R. W.; Schluter, M.; Sham, L. J. Trends in Self-Energy Operators and their Corresponding Exchange-Correlation Potentials. *Phys. Rev. B,* **1987**, *36*, 6497–6500; (b) Okoye, C. M. I. Theoretical Study of the Electronic Structure, Chemical Bonding and Optical Properties of $KNbO_3$ in the Paraelectric Cubic Phase. *J. Phys.: Condens. Matter,* **2003**, *15*, 5945–5958; (c) Terki, R.; Bertrand, G.; Aourag, H. Full Potential Investigations of Structural and Electronic Properties of $ZrSiO_4$. *Microelectron. Eng.,* **2005**, *81*, 514–523.